Automatic Data Extraction based on Semiconductor Datasheet for Design Automation of Power Converters

Fanghao Tian[1*], Diego Bernal Cobaleda[1], Wilmar Martinez[1]
1 Dept of Electrical Engineering (ESAT), KU Leuven-Energyville, Diepenbeek-Genk, Belgium
*E-mail: fanghao.tian@kuleuven.be

***Abstract*—The application of artificial intelligence (AI) to design automation (DA) is a novel research area in power electronics, owing to the complexity of power converter design, power loss modeling on magnetic and semiconductors, and the large number of components to choose from. This paper presents a tool for extracting dynamic and complex nonlinear characteristics from semiconductor datasheets in order to improve the power loss estimation model, resulting in an optimal power converter design. An object recognition neural network, CenterNet, is trained to extract figures from data-sheets. The dynamic data is then extracted from figures utilizing Optical Character Recognition (OCR) and morphological image processing techniques. Finally, the acquired data is used to augment the dynamic properties of power switches and to develop a more accurate power loss model for use as input to design automation tools.**

Keywords*—*Artificial Intelligence, design automation, image processing, power converters,

I. Introduction

With the development of decarbonized systems, such as electric cars, electric aviation, and photo-voltaic system, the demand for power electronic converters has increased significantly due to their widespread applications [1]. Increasingly strict requirements for the design of power converters in terms of efficiency, power density, volume, and mass are proposed [2]. However, designing optimal power converters is difficult due to the abundance of available power electronics components [3]. Furthermore, as it is impossible to test each design experimentally and choose the one with optimal performance, preselection of devices and simulations of the possible designs become necessary. Semiconductors simulations are frequently based on a simplified model which does not take into account all of the semiconductors' dynamic characteristics. Thus, it is critical to enhance the accuracy of the semiconductor loss calculation model in order to perform reliable power converter design optimization.

The study on information extraction has made some progress as the deep learning technique develops. Clark and Divvala proposed a method for detecting chunks of body text and locating the figures or tables by reasoning about empty regions [4] [5]. Siegel et al. proposed FigureSeer, an end-to-end framework for automatically locating figures in academic papers, particularly those with subfigures, and classifying them into figures in the result section and other sections using Convolutional Neural Networks (CNNs). Then, using Optical Character Recognition (OCR) algorithms that recognize text contained within figures such as titles and legends, all information contained within the figures is extracted [6]. Another powerful tool named Diag2graph was proposed in [7]. The same algorithm for figure localization as [6] was used. Various components such as node, text, and arrow were detected during the figure content analysis. Additionally, their relations are analyzed. ChartOCR in [8] is a universal model that extracts key point information and determines the chart type at the same time, then predicts the data range and extracts the text using Microsoft OCR. The extraction of data from line charts was studied in [9], while the segmentation of multiple curves was explored in color plots.

There are few tools especially for data extraction from power electronics data-sheets. In comparison to standard academic papers, data-sheets have several distinguishing characteristics. (1) There are intensive figures on some pages. (2) Some figures are in grayscale while others are in color. (3) The figures are line charts and usually have grids. On this basis, a special object recognition algorithm focusing on complex line charts in data-sheets is developed to extract data with high accuracy. This paper focuses on creating an AI-based tool to extract information from figures of semiconductors data-sheets to develop a method to improve semiconductors power loss calculation modeling for simulation in power converter design automation.

The paper is organized as follows. In section II, A CenterNet-based object detection algorithm is utilized to detect and separate the figures from data-sheets. In section III, the same neural network with differently trained weight parameters is implemented for the figures' key elements detection. Combined with the results of text recognition by OCR, data from line charts are extracted. Then, the power loss model of power switch is enriched by the obtained dynamic data in section IV. The results and conclusion are in section V and section VI separately.

II. Figure Separation

A. Task Overview

To automate the data extraction process from data sheets, it is necessary to separate the figures in the data sheets prior to conducting figure analysis. Image

processing algorithms are used to extract data from each separate figure. Object detection, text recognition, and line data extraction are the primary tasks. The flowchart is as shown in Fig.1.

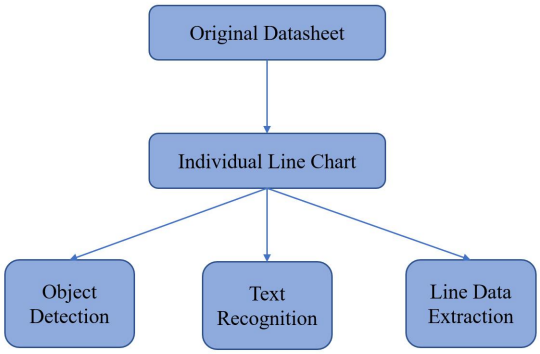

Fig. 1: Overview of data extraction task.

Detailed procedures for figures separation will be described as follows.

B. Dataset Establishment

The positions of figures are recognized using a CNN-based object detection algorithm. Therefore, pages of transistor data-sheets are collected to construct the dataset for training by manually annotating original data-sheet pages. An example of the annotated page is as shown in Fig.2, where figures on the data-sheet page are annotated with a figure label.

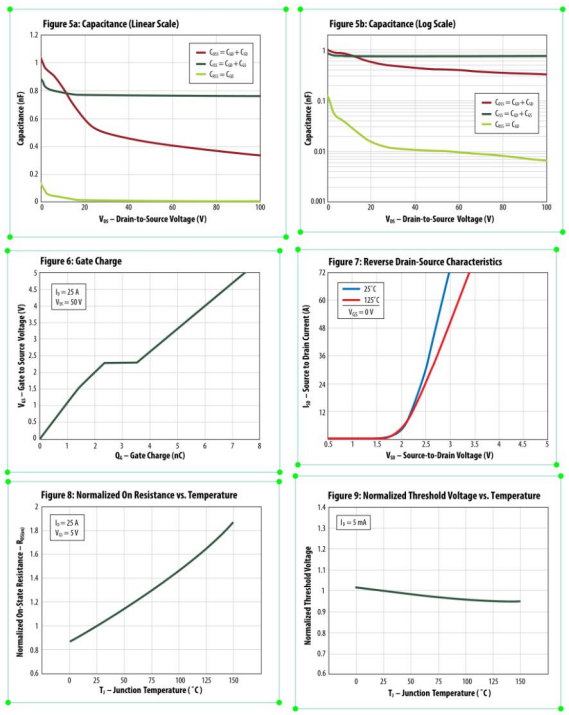

Fig. 2: Examples of annotated page [10].

Different manufacturers' data-sheets have a variety of different styles. Notably, some pages contain six figures, while others may only contain four. Additionally, figures sometimes occupy only a portion of the page. To increase the object detection algorithm's universality, data-sheets from several different manufacturers are gathered. Different data-sheets from the same manufacturer, on the other hand, have a similar layout. As a result, CNN training requires only a small amount of training data.

C. CenterNet

Object detection is a challenging task in computer vision. Numerous algorithms have been developed, such as YOLO, RCNN, Faster RCNN and etc [12]. CenterNet is a novel anchor-free object detection algorithm with good performance for object detection on multiple scales [11]. To begin, a multiple layer deep CNN network serves as the backbone for feature extraction from original pictures. Corner pooling and center pooling are implemented on top of the backbone to obtain two corner heatmaps and a center key point heatmap, which detect a pair of corners and a center, respectively, thus determine the bounding box for the object. The architecture of CenterNet is shown in Fig.3.

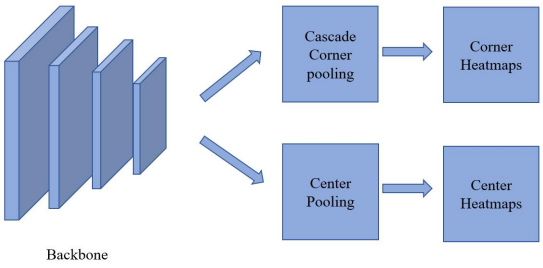

Fig. 3: Architecture of CenterNet.

The choice of backbone CNN is determined by the complexity of dataset. Due to the similarity of data-sheets pages and figures, ResNet50 is chosen to be the backbone CNN [13].

D. Training

Following the preparation of the labeled dataset and the CenterNet algorithm, the training for 100 epochs begins. A frozen scheme is used to speed up the training process. Firstly, a well-trained ResNet50 model by a large classic dataset is loaded, the parameters of which stay unchanged for the first 50 training epochs. The training process is then continued with the ResNet50 parameters unfrozen. The labeled pages are randomly divided into training and validation dataset with percentages of 90% and 10%, respectively.

III. Data Extraction

Individual figures are separated from data-sheets and analyzed to extract detailed information. Similar to the figure separation task, object detection is the initial step in locating and recognizing the critical elements of a figure, such as the title, legend, coordinate origin corner,

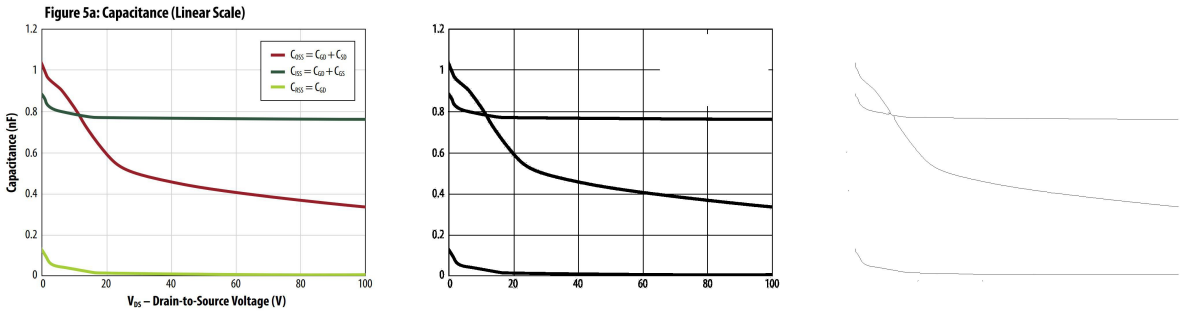

(a) (b) (c)

Fig. 4: Line extraction process (a) original image. (b) binarized image. (c) line skeleton.

label, and values of x-axis and y-axis marks. Then text recognition is required to identify text and numbers, which are required to comprehend figure information. Finally, the line data with correct coordinate values are extracted.

A. Dataset Establishment

To train the CenterNet for line chart recognition, a dataset must be constructed by manually annotating figures cut from transistor data-sheets. Six key elements are indicated, which are title, legend, label, value, corner, and other (if exists). Similarly, in order to increase the universality of the algorithm, figures in a variety of styles from a variety of manufacturers are gathered. And they are randomly divided into training and validation datasets with percentages of 90% and 10%, respectively. An example of the annotated figure is as shown in Fig. 5.

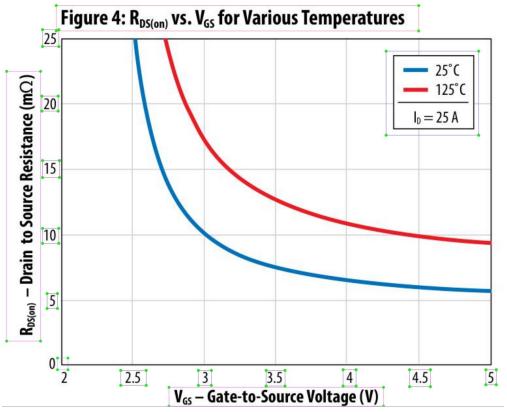

Fig. 5: Example of annotated figure [10].

The same CenterNet is trained by the line chart dataset for 100 epochs.

B. Data Extraction

After recognizing the key elements of figures, data can be extracted by text recognition and line data processing.

1) Text recognition: Optical character recognition (OCR) has been developing dramatically recently. Tesseract, an open-source OCR engine, is utilized in this paper. Combined with label information from object detection, recognized texts are classified as title, label and etc.

2) Line data extraction: Prior to digitizing data in a line chart, it is necessary to specify the coordinate information along with the mark values. To begin, recognized values are classified into x-axis and y-axis values. Then, because the majority of data-sheet figures contain grids, the figure is binarized to detect vertical and horizontal lines that correspond to mark values. In this way, an accurate coordinate is established.

The following step is to remove the background grid and extract data from individual lines. Since the lines are generally thicker than the grid, morphological image processing techniques are applied to eliminate the grid. More specially, morphological closing, which is a dilation operation followed by an erosion, is implemented to remove the thin black grid on the background. Then the skeleton of lines is extracted to reduce line width into a single pixel, making data extraction easier.

Finally, for line charts with multiple lines, an additional step of data correlation is required. After collecting all pixel coordinates, they are grouped according to their x axis values, like $[(x_i, y_{i1}), (x_i, y_{i2}), \cdots, (x_i, y_{in})]$. The next dot can be estimated using the coordinates of the previous two dots on a line as 1:

$$\hat{y}_{i+1} = \frac{y_i - y_{i-1}}{x_i - x_{i-1}}(x_{i+1} - x_i) + y_i \tag{1}$$

Then the dot closest to $\hat{y}_{i+1}$ is considered to be the correlated dot for this line. And to prevent incorrect correlation or noise interference, the distance between the estimated position and the closest dot is limited to a specific range.

The process of converting the original figure to a binarized figure for the purpose of matching mark values, then to a line skeleton for the purpose of extracting line data is illustrated in Fig. 4. The title and labels are removed during the binarization process to eliminate background noise.

IV. Analytical Semiconductor Power losses Model

In the power electronics design process, the selection of semiconductors components significantly impacts the performance of power converters. Traditionally, engineers tend to choose the components based on experiences since It is impractical to manually inspect thousands of semiconductor components, and the market is filled up with semiconductor switching devices with similar voltage and current characteristics. As a result, additional time is spent selecting a device. Additionally, the parameters and variables of semiconductors are highly relevant. To be able to determine which of them, or which combination of them will improve the overall efficiency of the converter, an accurate and fast model is required. However, dynamic data from data-sheets can improve the analytical power loss model on field effect transistor (FET) to get a more precise estimation model. Thus, power converter designs can be thoroughly evaluated and optimized.

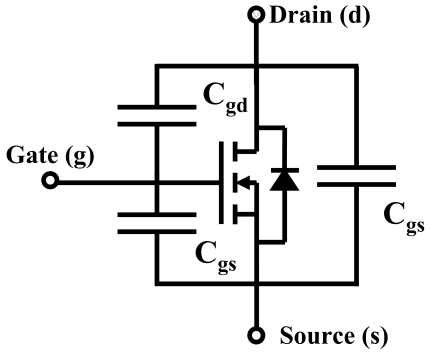

Fig. 6: FET capacitances.

Fig.6 Shows the representation of the intrinsic capacitance of a conventional FET. Where; input capacitance C_{iss}=$C_{gd}+C_{gs}$, output capacitance C_{oss}=$C_{ds}+C_{gd}$, and reverese transfer capacitance C_{rss}=C_{gd}.

A. Power Loss model

Power losses on semiconductor switches, generally consist of conduction losses, gate losses, switching losses and reverse recovery losses. To estimate them, common used calculation models are shown in (2)-(5) [15]. Additionally, when calculating power loss, the parameters in these formulations are typically fixed to typical values rather than dynamic data from data-sheet plots, which implies a more accurate behavior of the device. In Fig. 7 two screenshots from a power FET are shown, Fig. 7a depicts the typical parameters usually taken for the design while Fig. 7b depicts the behaviour of the dynamic parameters depending on the operation point of the FET.

$$P_c = R_{DS(on))}\ {I_{D_{RMS}}}^2 \tag{2}$$

$$P_g = C_{iss} V_{GS}^2 f_s \tag{3}$$

$$P_{sw} = \frac{V_{DS} I_D}{2}(t_r + t_f) f_s \tag{4}$$

$$P_{rr} = C_{oss} V_{DS}^2 f_s \tag{5}$$

where t_r and t_f are turning on and turning off time, which can be calculated by formulations in [16].

Dynamic Characteristics (T_J = 25°C unless otherwise stated)						
PARAMETER		TEST CONDITIONS	MIN	TYP	MAX	UNIT
C_{ISS}	Input Capacitance	V_{DS} = 50 V, V_{GS} = 0 V		770	900	pF
C_{OSS}	Output Capacitance			430	650	
C_{RSS}	Reverse Transfer Capacitance			10	15	
R_G	Gate Resistance			0.3		Ω
Q_G	Total Gate Charge	V_{DS} = 50 V, V_{GS} = 5 V, I_D = 25 A		7.5	9	nC
Q_{GS}	Gate-to-Source Charge	V_{DS} = 50 V, I_D = 25 A		2.4		
Q_{GD}	Gate-to-Drain Charge			1.2	2	
$Q_{G(TH)}$	Gate Charge at Threshold			1.6		
Q_{OSS}	Output Charge	V_{DS} = 50 V, V_{GS} = 0 V		31	45	
Q_{RR}	Source-Drain Recovery Charge			0		

All measurements were done with substrate connected to source.
Note 2: $C_{OSS(ER)}$ is a fixed capacitance that gives the same stored energy as C_{OSS} while V_{DS} is rising from 0 to 50% BV_{DSS}.
Note 3: $C_{OSS(TR)}$ is a fixed capacitance that gives the same charging time as C_{OSS} while V_{DS} is rising from 0 to 50% BV_{DSS}.

(a)

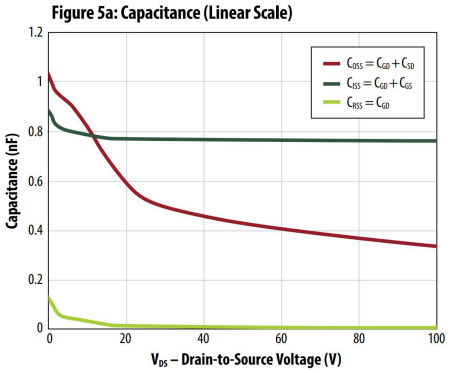

(b)

Fig. 7: Parameters for power loss calculation from data-sheets (a) Typical parameter values (b) Dynamic values [10].

B. Improved power loss model

. As previously stated, dynamic data from data-sheets are extracted and stored, which can be used to augment the model for calculating power loss. For conduction loss formulation (2), conventional method is to choose a fixed value for $R_{DS(on)}$. However, according to data-sheets, conduction resistance is a variable that is dependent on the junction temperature. As a result, the specific value of turn on resistance should be determined by the temperature. A dynamic conduction loss map is shown as Fig. 8 with junction temperature and drain current changing between $[0-150]$ and $[0-50]$ separately.

For reverse recovery loss (5), the output capacitance C_{oss} is a variable depending on drain to source voltage V_{DS} as is shown in 7b. Instead of regarding C_{oss} as a constant, an improved calculation method is shown in (6). The integration can be estimated by data from the line chart.

$$P_{rr}^{'} = V_{DS} f_s \int_0^{V_{DS}} C_{oss} V dV \tag{6}$$

As for the switching loss (4), similar dynamic data can be implemented in the process of calculating t_r and t_f.

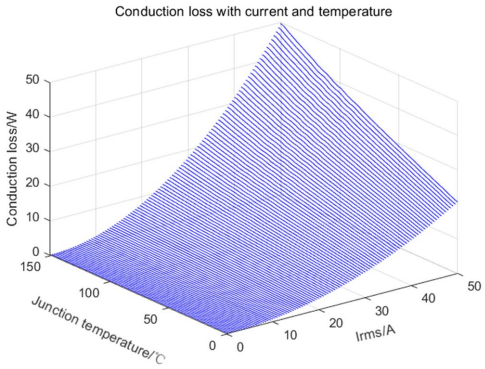

Fig. 8: Conduction loss with RMS current and junction temperature.

V. Results

A total of 200 pictures for the figure separation task and 300 pictures for the line data extraction task have been trained and tested. As is shown in Fig. [**?**], the training loss reduces dramatically and stays at a small value. The final training losses are 2.59 and 0.87 for both tasks, while the validation losses are 2.15 and 0.57 separately.

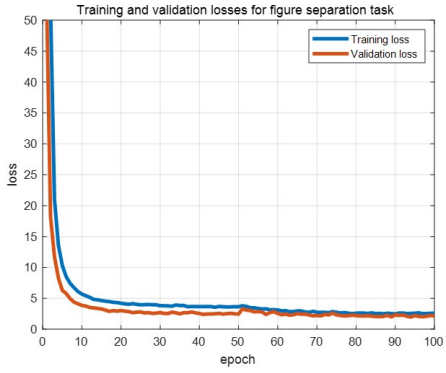

(a)

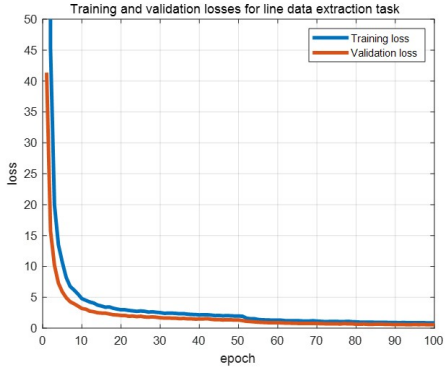

(b)

Fig. 9: Training and validation losses for (a) figure separation (b) line data extraction.

With the small training and validation losses, the trained CenterNet can detect the key elements from a data-sheet page or line chart. Two examples of the results are illustrated in Fig. 10a. Every figure on this page is detected and selected by the red bounding boxes. With the bounding box information, the figures can be cut into individual figures. Additionally, for the line chart data extraction task, 10b displays the critical elements highlighted by bounding boxes and classified according to the pre-defined classes. After applying the OCR for text recognition and traditional image processing algorithms for curve extraction, the dynamic data are extracted from data-sheets successfully.

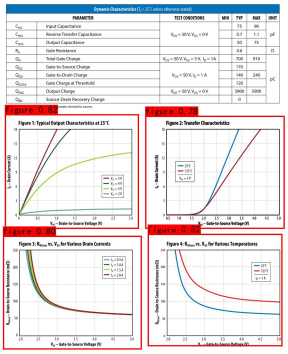

(a)

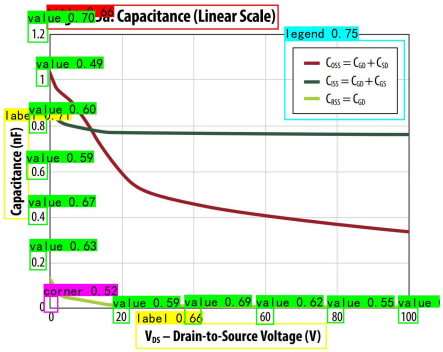

(b)

Fig. 10: Object detection results for (a) figure separation (b) line data extraction [10].

VI. Conclusions

Power loss simulation is critical for power electronics DA. Semiconductor components like power FETs have inevitable power loss, especially at high frequencies. Thus, a precise mathematical model of semiconductor power loss can result in the optimal selection of a semiconductor component for a particular design requirement. By acquiring dynamic data from data sheets, it is possible to accurately estimate the power loss of a specific component under specified operating conditions.

In this paper, a CenterNet based tool for data extraction of semiconductors data-sheets is proposed. Firstly, CenterNet was trained for two tasks, which are figure

separation from original data-sheets and key elements recognition for line charts. Secondly, data extraction from line charts is accomplished using image processing techniques. Finally, an improved dynamic power loss model is explained, considering junction temperature for conduction loss and dynamic intrinsic capacitance for reverse recovery loss. The same method can be utilized to enhance the switching loss model.

REFERENCES

[1] W. Martinez, C. Cortes, A. Bilal and J. Kyyra, "Finite Element Methods for Multi-objective optimization of a High Step-up Interleaved Boost Converter," in 2018 International Power Electronics Conference (IPEC-Niigata 2018 -ECCE Asia), pp. 2193-2198, 2018,

[2] W. Martinez, M. Yamamoto, J. Imaoka, F. Velandia and C. A. Cortes, "Efficiency optimization of a two-phase interleaved boost DC-DC converter for Electric Vehicle applications," in 2016 IEEE 8th International Power Electronics and Motion Control Conference (IPEMC-ECCE Asia), pp. 2474-2480, 2016.

[3] Mouser Electronics. Accessed on: October 10, 2021. [Online]. Available: https://eu.mouser.com/c/semiconductors/discrete-semiconductors/

[4] C. Clark and S. Divvala. "Looking Beyond Text: Extracting Figures, Tables, and Captions from Computer Science Papers," in AAAI Workshops at the Twenty-Ninth AAAI Conference on Artificial Intelligence, pp. 2-8, 2015.

[5] C. Clark and S. Divvala. "PDFFigures 2.0: Mining figures from research papers," in 2016 IEEE/ACM Joint Conference on Digital Libraries, pp. 143-152, 2016.

[6] N. Siegel, Z. Horvitz, R. Levin, S. Divvala, and A. Farhadi, "Figureseer: Parsing result-figures in research papers," in European Conference on Computer Vision, pp. 664–680, 2016.

[7] A. Roy, I. Akrotirianakis, A. Kannan, D. Fradkin, A. Canedo, K. Koneripalli, and T. Kulahcioglu. "Diag2graph: Representing Deep Learning Diagrams in Research Papers as Knowledge Graphs," in 2020 IEEE International Conference on Image Processing (ICIP), pp. 2581-2585, 2020.

[8] J. Luo, Z. Li, J. Wang and C. -Y. Lin, "ChartOCR: Data Extraction from Charts Images via a Deep Hybrid Framework," in 2021 IEEE Winter Conference on Applications of Computer Vision (WACV), pp. 1916-1924, 2021.

[9] S. Choudhury, S. Wang, P. Mitra, and C. Giles, "Automated data extraction from scholarly line graphs," in Eleventh IAPR International Workshop on Graphics Recognition (GREC), 2015.

[10] EPC Products data-sheets. Accessed on: February 28, 2022. [Online]. Available: https://epc-co.com/epc/Products/eGaNFETsandICs.aspx

[11] K. Duan, S. Bai, L. Xie, H. Qi, Q. Huang and Q. Tian, "CenterNet: Keypoint Triplets for Object Detection," in 2019 IEEE/CVF International Conference on Computer Vision (ICCV), pp. 6568-6577, 2019.

[12] L. Jiao, F. Zhang, F. Liu, S. Yang, L. Li, Z. Feng, and R. Qu, "A Survey of Deep Learning-Based Object Detection", IEEE Access, vol. 7, pp. 128837–128868, 2019.

[13] K. He, X. Zhang, S. Ren and J. Sun, "Deep Residual Learning for Image Recognition," 2016 IEEE Conference on Computer Vision and Pattern Recognition (CVPR),pp. 770-778, 2016.

[14] R. Smith, "An Overview of the Tesseract OCR Engine," Ninth International Conference on Document Analysis and Recognition (ICDAR 2007), pp. 629-633, 2007.

[15] Z. J. Shen, Y. Xiong, X. Cheng, Y. Fu and P. Kumar, "Power MOSFET Switching Loss Analysis: A New Insight," Conference Record of the 2006 IEEE Industry Applications Conference Forty-First IAS Annual Meeting, pp. 1438-1442, 2006.

[16] Vishay Siliconix, Appl. Note AN608A, pp.1-6. Available: https://www.vishay.com/docs/73217/an608a.pdf